TOA Estimation Technique for IR-UWB Based on Homogeneity Test

Mustapha Djeddou, Hichem Zeher, Younes Nekachtali, and Karim Drouiche

This paper deals with the estimation of the time of arrival (TOA) of ultra-wideband signals under IEEE 802.15.4a channel models. The proposed approach is based on a randomness test and consists of determining whether an autoregressive (AR) process modeling an energy frame is random or not by using a distance to measure the randomness. The proposed method uses a threshold that is derived analytically according to a preset false alarm probability. To highlight the effectiveness of the developed approach, simulation setups as well as real data experiments are conducted to assess the performance of the new TOA estimation algorithm. Thereby, the proposed method is compared with the cell averaging constant false alarm rate technique, the threshold comparison algorithm, and the technique based on maximum energy selection with search back. The obtained results are promising, considering both simulations and collected real-life data.

Keywords: TOA estimation, IR-UWB, localization, homogeneity test, energy detectors.

I. Introduction

Impulse radio ultra-wideband (IR-UWB) has many interesting features that can be used to achieve accurate temporal resolution to allow localization around a few decimeters [1]. The IR-UWB technology is a serious candidate for various applications, such as radar detection, short-range wireless, and many other emerging technologies.

Among methods used to locate a radio source, we cite received signal strength, time difference of arrival (TDOA), angle of arrival, and time of arrival (TOA) [2]. We highlight that synchronization algorithms for IR-UWB [3] share some common threads with TOA algorithms, but, as the goals are different, we focus only on TOA algorithms.

We can classify TOA estimation into two main categories, depending upon the type of used receivers. There are correlation receivers or matched filter (MF) receivers and energy detection (ED) receivers. In the MF-based detection, a high sampling rate is used to allow precise localization. However, this is done at the expense of a high implementation complexity. On the other hand, ED-based receivers are easy to implement and consume less energy, but the accuracy depends on the sampling rates [4]. The approach developed in this paper belongs to this class.

The principle of the used receiver is sketched out in Fig. 1. At the output of the antenna, the signal is amplified by a low-noise amplifier (LNA). Then, the signal passes through a bandpass filter. In ED receivers, the filtered signal goes through a squaring device, and discrete samples are then obtained at a low frequency rate ($1/T_b$) at the output of an integration block. The estimated TOA depends on a predetermined threshold [5].

An MF-receiver-based algorithm that searches the maximum correlation between the received signal and the replica of the

Manuscript received Dec. 30, 2012; revised Apr. 10, 2013; accepted Apr. 18, 2013.

Mustapha Djeddou (phone: +213 555 475 704, djeddou.mustapha@gmail.com), Hichem Zeher (zeher.hichem@hotmail.fr), and Younes Nekachtali (nekachtali.younes@hotmail.fr) are with the Communication Systems Laboratory, Military Polytechnic School, Algiers, Algeria.

Karim Drouiche (kd@ptm.u-cergy.fr) is with LPTM, Cergy University, Paris, France.

http://dx.doi.org/10.4218/etrij.13.0112.0889

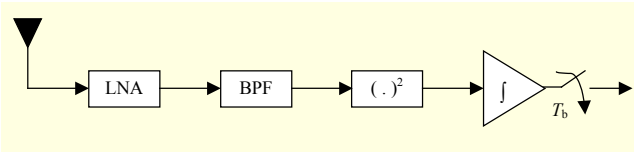

Fig. 1. UWB receiver based on energy detector.

transmitted signal was presented in [6]. The generalized maximum likelihood [7], which is an improved version of the CLEAN algorithm, is another MF-receiver-based algorithm.

Many algorithms based on ED receivers can be found throughout the literature. The concept of TOA estimation consists of finding the first block containing the energy of the received signal. Another way to estimate TOA is to compare each block with suitable threshold energy (threshold comparison [TC] algorithm) [5]. As the name implies, the maximum energy selection with search back (MESSB) technique is the MES technique modified by adding a search back step [8]. Recently, the cell averaging constant false alarm rate (CA-CFAR)-based method [9], which is borrowed from the radar field, has been used to estimate TOA. This method is based on a comparison of the energy blocks with respect to an adaptive threshold while keeping a constant false alarm. The difficulty resides in determining the threshold, as it depends on experimental quantities. Other works consider two-step estimation, in which a coarse estimation is followed by an iterative-threshold-test-based fine time estimation, as proposed in [10]. Another drawback of ED-based approaches is that they rely upon finding the first incoming path rather than the strongest one. This problem arises especially in multipath channels.

In this paper, a new approach for estimating TOA is built. The proposed method mainly consists of performing a randomness test between two autoregressive (AR) processes involving an adequate distance measure. In addition, it is worthy to point out that the involved threshold is fixed analytically, and the detection probability is fully expressed.

The paper is organized as follows. Section II presents the data model and the main hypotheses used throughout the paper. Section III focuses on the proposed method. Section IV addresses the conducted simulation and the real-life data to assess the performance of the developed approach. Section V concludes the paper.

II. Data Model

In IR-UWB systems, the received signal can be expressed as

$$R(t)=\sum_{i=-\infty}^{+\infty} b_i w_{\mathrm{rs}}\left(t-iT_{\mathrm{sym}}\right)+n(t), \tag{1}$$

where b_i is the information bit, i is the index of the symbol, T_{sym} is the symbol duration, and $n(t)$ is additive white Gaussian noise (AWGN) with zero mean and two-sided power spectral density $\frac{N_0}{2}$. The waveform of the received symbol is $w_{\mathrm{rs}}(t)$, given by the following expression:

$$w_{\mathrm{rs}}(t)=\sum_{j=0}^{N_{\mathrm{f}}-1} w_{\mathrm{R}}(t-jT_{\mathrm{f}}-c_jT_{\mathrm{c}}), \tag{2}$$

where N_{f} is the number of frames per symbol, T_{f} and T_{c} respectively refer to the frame duration and the chip duration, and $\{c_j\}$ are the time hopping codes used to mitigate interferences between multiple users ($c_j \in \{0,\ldots,N_{\mathrm{c}}-1\}$, where N_{c} stands for the number of chips per frame). Finally, $w_{\mathrm{R}}(t)$ is the received pulse waveform defined as

$$w_R(t)=\sum_{l=1}^{L}\alpha_l g(t-\tau_l), \tag{3}$$

where $\{\alpha_l,\tau_l\}$ are the attenuation and the delay of the i-th path, respectively, $g(t)$ is the waveform of the transmitted signal, L is the number of paths, $\tau_{\mathrm{TOA}}=\tau_1$ is the delay of the first path, and $\tau_{\mathrm{TOA}} \sim U(0,T_{\mathrm{f}})$ with $U(\cdot)$ is the uniform distribution.

For now, we assume to have two frames, $X(n)$ and $Y(n)$, collected from the sampled version of $R(t)$ to perform the estimation. Vectors $X(n)$ and $Y(n)$ are N-dimensional vectors modeled by AR processes of order, p_x and p_y, respectively.

The two frames must be kept separate by V samples to ensure that the independent and identically distributed (i.i.d.) property holds between the two processes. Depending on the presence or not of IR-UWB signals, $X(n)$ and $Y(n)$ may be signal-free frame (only noise) or noise plus signal frame. We try to find a way to detect the change of the statistical behavior of the two processes.

III. Proposed Approach

In this section, we derive a procedure to estimate the TOA. We suppose that $X(n)$ contains blocks of samples' energy instead of the samples' values.

Let the two AR processes, $X(n)$ and $Y(n)$, be expressed as

$$X(n)=-\sum_{k=1}^{p_x} a_X(k)X(n-k)+u_X(n), \tag{4}$$

$$Y(n)=-\sum_{k=1}^{p_y} a_Y(k)Y(n-k)+u_Y(n), \tag{5}$$

where $u_X(n)$ and $u_Y(n)$ are white noise, centered, i.i.d., with variances σ_X^2 an σ_Y^2, respectively. $\left[a_X(1),a_X(2),\cdots,a_X(p_x)\right]$ and $\left[a_Y(1),a_Y(2),\cdots,a_Y(p_y)\right]$ are the coefficients of the AR

models.

We choose AR modeling due to its superiority over many other methods, as it can take advantage of the intrinsic noise found in received UWB signals, and it can extract meaningful information from propagation of that noise in the signal. Secondly, AR modeling can be used in the calculation of a power spectrum density instead of the discrete Fourier transform (DFT), as it provides a smoother power spectrum compared to the DFT and is hence more convenient to interpret. Furthermore, the frequency resolution of the estimated signal spectrum can be provided more precisely than with the DFT and is not affected by the length of the used sequence of data.

Basically, the AR model is based on a set of autocorrelation functions computed by multiplying a data sample $X(n)$ with a delayed version of itself. For a small delay, the values of the two delayed signals exhibit similarities. As the delay increases, the difference between the two data sequences becomes more noticeable. For the UWB received signals, the signal is a combination of periodic UWB pulse signals and random noise that progressively vanishes as the lag increases, which is useful for extracting signals with periodic behavior from random noise.

The autocorrelation functions of the processes are directly related to the coefficients of the AR model. This relationship is inverted to derive these coefficients via an autocorrelation function using Yule-Walker equations.

The Yule-Walker equations for the $X(n)$ AR process (same equation forms are obtained for $Y(n)$ process) are given by

$$\Gamma_X(l) = -\sum_{i=1}^{p_x} a_X(i)\Gamma_X(l-i) + \sigma_X^2 \delta(l,0), \tag{6}$$

where $l = 0,1,\ldots,p_x$, yielding p_x+1 equations. The autocorrelation function of X is Γ_l, and the Kronecker delta function is $\delta(l,0)$.

The coefficients a_X (and a_Y) are obtained using the Levinson-Durbin algorithm, which is a recursive method [11], [12]; it takes advantage of the Hermitian Toeplitz structure of the autocorrelation matrix.

The AR model is determined by the model order p_x and the prediction coefficients a_X, fitting the model to the data. The most used criterion for selecting p_x is Akaike's Information Criterion [13]. The following expression is used to compute the AR model order:

$$AIC(p_x) = N\ln\left(\sigma_x^2\right) + 2p_x, \tag{7}$$

where σ_x^2 is the prediction error variance associated with p_x.

The estimated parameters are then used to compute the power spectral densities, $S_X(f)$ and $S_Y(f)$, of $X(n)$ and $Y(n)$, respectively, by

$$S_X(f) = \frac{\sigma_X^2}{\left|P_X(f)\right|^2} = \frac{\sigma_X^2}{\left|1+\sum_{k=1}^{p_x} a_X(k)e^{-j2\pi fk}\right|^2}, \tag{8}$$

$$S_Y(f) = \frac{\sigma_Y^2}{\left|P_Y(f)\right|^2} = \frac{\sigma_Y^2}{\left|1+\sum_{k=1}^{p_y} a_Y(k)e^{-j2\pi fk}\right|^2}, \tag{9}$$

where $P_X(f)$ and $P_Y(f)$ are the powers of the AR models. We define $q(f)$ as the nonnegative ratio [14]:

$$q(f) = \frac{S_X(f)}{S_Y(f)} = \frac{\sigma_X^2}{\sigma_Y^2} \cdot \frac{\left|1+\sum_{k=1}^{p_y} a_Y(k)e^{-j2\pi fk}\right|^2}{\left|1+\sum_{k=1}^{p_x} a_X(k)e^{-j2\pi fk}\right|^2}. \tag{10}$$

We note that $S_X(f)$ and $S_Y(f)$ can be computed using other methods, such as the fast Fourier transform (FFT). The main purpose for adopting the AR approach is its ability to provide the same resolution as that provided by the FFT method, but with smaller sample sizes. Hence, the computational load is reduced because fewer samples are involved. This makes the AR approach advantageous, especially for real-time implementation.

In what follows, we use distance $D(S_X(f), S_Y(f))$ (denoted by $D(q)$) [14], which involves ratio $q(f)$ of spectral densities S_X and S_Y of $X(n)$ and $Y(n)$, respectively:

$$D(q) = \log\int_{-\frac{1}{2}}^{+\frac{1}{2}} q(f)df - \int_{-\frac{1}{2}}^{+\frac{1}{2}} \log q(f)df. \tag{11}$$

1. Homogeneity-Test-Based TOA Estimation

We determine, in this method, whether an AR signal, which models window blocks containing the energy of received samples, is a noise or not. The decision is made by comparing the result of an adequate special case of the distance measure in (11) to a threshold. This method is called HOmogeneity Test based EStimation of Time of arrival (HOTEST). Figure 2 shows the one sliding window mode used in the HOTEST algorithm context.

The used detector is an ED-based one, in which every cell represents an energy block of the received signal over the integration period T_b. Hence, the energy blocks $X(n)$, sampled at $\frac{1}{T_b}$, are evaluated using the following formula:

$$X(n) = \sum_{j=0}^{N_f-1} \int_{jT_f+(c_j+n)T_b}^{jT_f+(c_j+n-1)T_b} \left|R(t)\right|^2 dt. \tag{12}$$

The block index is denoted by $n \in \{1,2,\ldots,N_b\}$, and the number of blocks contained in the time frame T_f and half of the

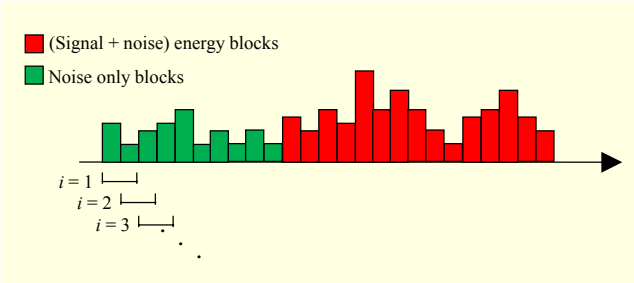

Fig. 2. Shifting window in HOTEST algorithm.

next frame is denoted by N_b.

In CA-CFAR-based TOA estimation [9], an expectation over K symbols can be taken to reduce the noise effect. However, in our proposed approach, the expectation operation does not allow for an improvement in performance, as the decision is carried out using a distance measure rather than using the average power level, as used in the CA-CFAR-based method. Therefore, we look for the index of the cell under test having the distance exceeding the pre-fixed threshold S_α. The winning temporal index corresponds to the estimated TOA.

At this stage, two options are available to us. The first option involves the use of two windows sliding together but separated by V samples to maintain the i.i.d. assumption. The spectrum of the two sequences is computed, and the distance in (11) is used to detect the change in the statistical behavior. In this case, it is a proportionality test between the two AR process models. The second option consists of considering the second window, $Y(n)$, as a "fictive" window containing energy of noise-only samples having constant variance. Hence, we are left with only sequence $X(n)$ to perform a test of homogeneity of the AR process modeling this window. In this work, we adopt the second approach because the computation is reduced by half.

In what follows, the AR process $Y(n)$ is supposed to be a white noise process with variance $\sigma^2 = h$.

$$\begin{aligned} q(f) &= \frac{S_X(f)}{S_Y(f)} \\ &= \beta\sigma_X^2 \left| 1 + \sum_{k=1}^{p_x} a_X(k) e^{-j2\pi fk} \right|^{-2} \\ &= \beta S_X(f), \end{aligned} \tag{13}$$

where β stands for constant variables. Using the propriety of distance invariance by homothety, we have

$$\begin{aligned} D(q(f)) &= D(\beta S_X(f)), \\ &= D(S_X(f)). \end{aligned} \tag{14}$$

Hence, the distance in (11) can be rewritten as follows:

$$D(q) = \log \int_{-\frac{1}{2}}^{+\frac{1}{2}} S_X(f)\, df - \int_{-\frac{1}{2}}^{+\frac{1}{2}} \log S_X(f)\, df. \tag{15}$$

Distance $D(q)=0$ if and only if $S_X(f)=h$, where h is an arbitrary positive constant. This property is the most important among the distance properties because it represents the essential tool for the proposed test.

Now, we formulate the statistic test. It is considered that if an AR process has a constant spectral density, the AR a_X parameter vector is the zero vector. In this case, we execute the test defined below to check the randomness of the AR process.

$$\begin{cases} H_0, & S_X(f) = h, \\ H_1, & S_X(f) \neq h. \end{cases} \tag{16}$$

So, the test is written as follows [14].

1) Under the non-null hypothesis, H_1, we have

$$N^{\frac{1}{2}} \left(\hat{D} - D \right) \rightarrow \mathcal{N}(0, \upsilon), \tag{17}$$

where υ is the variance of the normal distribution, D is the bias of the distance, and N stands for the window size.

2) Under the null hypothesis, H_0, $S_X(f) = h$; the test is written as follows:

$$\frac{N\hat{D} - n}{\sqrt{2n}} \rightarrow \mathcal{N}(0,1), \tag{18}$$

where n is a positive number such that $p_X < n < N$.

An important observation concerning (17) and (18), as reported in [14], is that the behavior of the statistic changes abruptly by a factor of $\sqrt{N}$ when moving from H_1 to H_0 or vice versa. This is a crucial property that helps in the detection of the changes of the statistical model of the frame under test when it slides over time.

Having the distributions under the two hypotheses, we may use the Neyman-Pearson formalism to go through hypothesis testing. The false alarm probability is set to a fixed value (α= 5% or 1%):

Now, the probability of detection can be provided by taking into account the distributions of statistics under both hypotheses. In this case, we use the statistic $\widehat{D}$. So, the probability of false alarm α is written as follows [14]:

$$P_{H_0}\left(\frac{N\hat{D} - n}{\sqrt{2n}} \geq S_\alpha \right) = \alpha. \tag{19}$$

We obtain the probability of detection:

$$P_d = P_{H_1}\left(\frac{N\hat{D} - n}{\sqrt{2n}} \geq S_\alpha \right). \tag{20}$$

Threshold S_α can be calculated using (19) and the inverse cumulative density function of normal distribution. A more convenient way may be adopted by using a lookup table of percentiles of the normal distribution. The time index of the

statistic $\frac{N\hat{D}-n}{\sqrt{2n}}$ that exceeds the threshold S_α represents the index of the estimated TOA.

The following algorithm summarizes the HOTEST approach:

Algorithm 1. HOTEST steps.
Inputs: False alarm probability α (typically set to 5%), N_b, T_b, and the window size N;
Output: Estimated TOA $\hat{\tau}_d$;
For $n = 1 : N_b$
  Compute sample energy blocks $X(n)$ using (12);
End for
  $i = 0$; % Frame Initialization
While $i \le N_b$
  Select a sliding window of size N;
  Estimate the AR model order p_X (optional operation, can be preset);
  Estimate the parameter vector a_X and the noise variance σ_X^2 using the Levinson-Durbin algorithm;
  Compute $S_X(f)$ and D according to (8) and (15);
  Determine the threshold S_α using lookup table values of normal distribution;
  If $D(i) > S_\alpha$
    $\hat{\tau}_d = (i - 0.5) * T_b$;
  Else
    $i = i + 1$;
  End if
End While
Return $\hat{\tau}_d$

IV. Experiment Results

1. Simulation Experiments

In this section, we deal with the performance of the proposed method. The adopted comparison criterion is the root mean squared error (RMSE) of the estimate versus the signal-to-noise ratio (SNR):

$$\hat{\tau}_{\mathrm{TOA}} = \sqrt{\frac{1}{K}\sum_{k=1}^{K}(\hat{\tau}_{\mathrm{TOA}}(k) - \tau_{\mathrm{TOA}}(k))^2}, \qquad (21)$$

where $\hat{\tau}_{\mathrm{TOA}}(k)$ is the k-th estimate of TOA, $\tau_{\mathrm{TOA}}(k)$ is the true TOA value, and K is the number of Monte Carlo runs, fixed to 1,000 for each experiment. An IR-UWB signal with the following properties is generated, modulated using pulse position modulation: T_f = 8 ns, T_{svm} = 40 ns, and sampling frequency $F_s = 1/T_s = 8$ GHz. The propagation channel is the IEEE802.15.4a, and the model is CM1: residential LOS. The frame size is set to N equals the duration of one pulse (N = 17 samples). The false alarm probability is set to α = 5%. The SNR is varied, and the RMSE is evaluated.

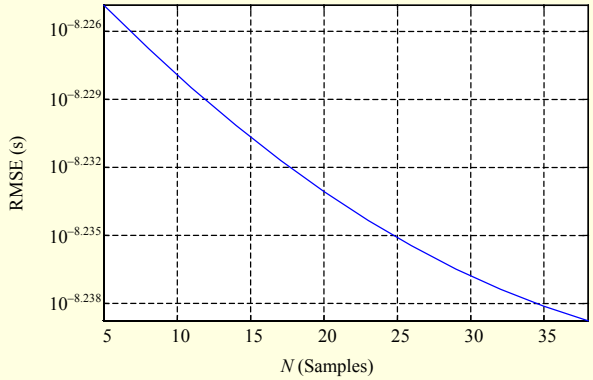

Fig. 3. Window length influence.

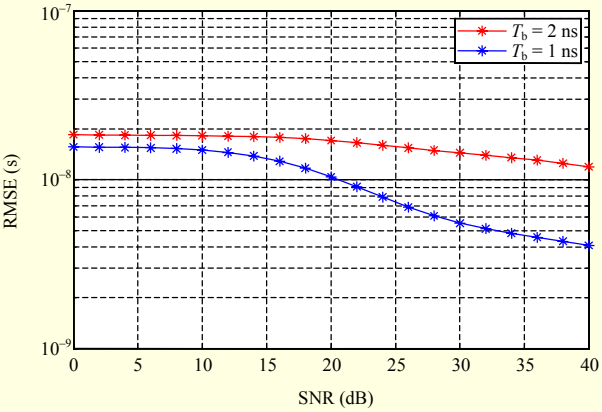

Fig. 4. T_b influence.

We first check the influence of the parameter N by varying its values between 5 and 40 samples. The SNR is set to 15 dB, T_b = 1 ns, and N_b = 50. As depicted in Fig. 3, the wider the window, the less the RMSE. The increase of the number of samples makes the estimation of the AR model parameters more accurate, and the distinction between noise-only frames and the signal-plus-noise frames becomes clearer. Next, we see the impact of varying the block duration. We take T_b = {1 ns, 2 ns}, and the SNR is varied within the interval of 0 dB to 40 dB. We notice, as shown in Fig. 4, that with the reduction of the sampling period the precision of the estimation increases. This is a predictable result, as the estimation error variance depends directly upon the sampling rate.

In what follows, we compare HOTEST to the CA-CFAR algorithm, the TC algorithm, and the MESSB algorithm using the same simulation conditions to prove the effectiveness of our approach in estimating TOA. The comparison is done under the following conditions.

- Fix $P_{fa} = \alpha = 0.05$ for the CA-CFAR and HOTEST algorithms.

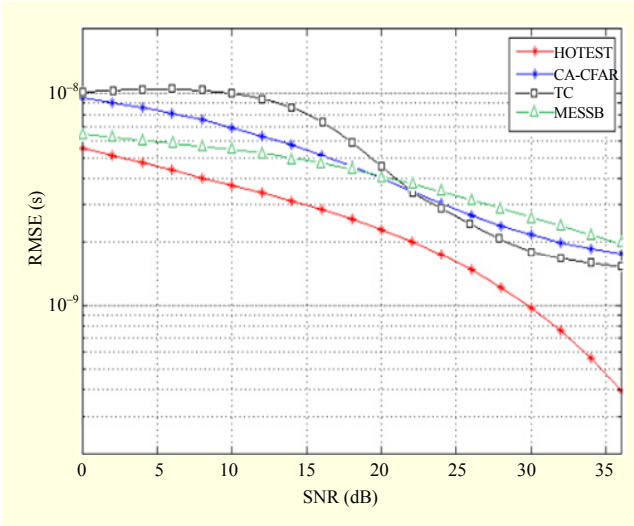

Fig. 5. Performance comparison: HOTEST vs. CA-CFAR, TC, and MESSB algorithms.

- N_b=100, N_g=40, T_b=1 ns with T=0.019 for the CA-CFAR algorithm.
- N=17, T_b=1 ns, N_b=100 for the HOTEST algorithm.

For the TC and MESSB algorithms, the normalized threshold is set to $\xi_n = 0.4$ and the searched back window is set to ω_s =30 ns.

Figure 5 shows that the HOTEST algorithm is superior to the other algorithms in terms of performance for all SNR values. We think that the HOTEST algorithm is superior as a result of the manner in which the statistical test is constructed. In fact, the proposed method does not depend directly on the values of the samples but on the distance measured by detecting an abrupt change.

In what follows, we study the influence of the NLOS environment when the HOTEST algorithm is used. For this, we set the following parameters: N=17, T_b=1 ns, N_b=100, and the SNR is varied between 0 dB and 36 dB. As shown in Fig. 6, in the absence of a direct path, the performance of HOTEST decreases in the CM2 model, but the achieved performance is still acceptable.

2. Real Data Experiments

In this section, we operate according to a real data experiment carried out by [15]. The application consists of locating a mobile transmitter. This operation involves the estimation of the TDOA.

We use evaluation kit PulsON 210, which consists of two tags (transmitter and receiver), and the transmission range can reach 6 m in an indoor environment and up to 150 m in free space, depending upon the transmission rate [16]. The technical characteristics of PulsON 210 are summarized below [17].

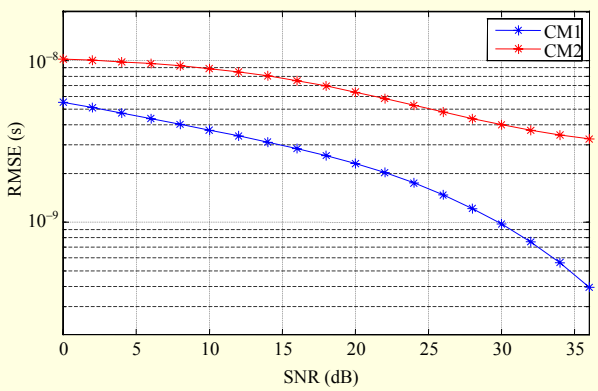

Fig. 6. CM1 vs. CM2 model using HOTEST algorithm.

Fig. 7. PulsON 210 transmitter/receiver.

- Repetition period (frame duration): 104.2 ns
- Transmission rate: 70 kbps - 9.6 Mbps
- Center frequency: 4.7 GHz
- Occupied band: 3.1 GHz - 6.3 GHz (B = 3.2 GHz)
- PIRE: −12.8 dBm
- Power consumption: 6.5 watts
- Dimensions: 16.5 cm × 10.2 cm × 5.1 cm

Furthermore, a system analysis module PulsON 210 can be exploited as a graphical tool for configuring, controlling, and receiving the data analysis.

The mobile transmitter and four receiver antennas are mounted on wooden supports of 1.5 m. The receiving antennas are connected to the receiver via coaxial cables and a PS4-7 combiner. In turn, the receiver is connected to a laptop through the Ethernet to transfer the received signals for processing. The objective is to measure TOAs; however, as the system is not synchronized, we measure the relative arrival time after the time difference is taken, to eliminate the unknown initial time t_0.

To track a mobile transmitter, many steps are necessary. First of all, the delays caused by electric coaxial cables must be estimated offline during the learning phase by using the *a priori* knowledge of the distances between the receiving antennas at the transmitter; see Fig. 8 for an illustrative scheme. The arrival time of the pulse to the i-th receiving antenna is then written as

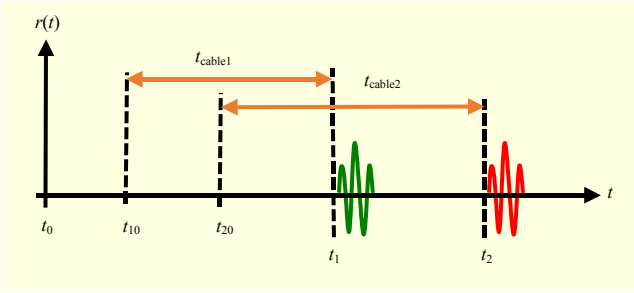

Fig. 8. Illustrative scheme of electrical delays in coaxial cables.

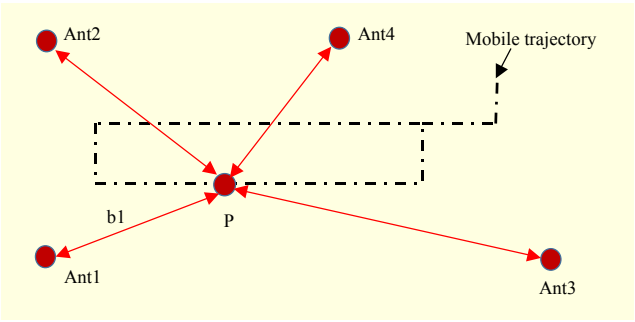

Fig. 9. Trajectory of mobile.

$$t_{i0} = t_i - t_{\text{cable}_i}, \tag{22}$$

where t_i is the arrival time of the pulse to the receiver, received by the i-th antenna. In fact, one can obtain, in our case, the equation of the TDOA as follows:

$$t_{20} - t_{10} = t_2 - t_1 - \left(t_{\text{cable}_2} - t_{\text{cable}_1}\right). \tag{23}$$

By setting $K_{21} = t_{\text{cable}_2} - t_{\text{cable}_1}$, (23) becomes

$$t_{20} - t_{10} = t_2 - t_1 - K_{21}. \tag{24}$$

Now, if we set $K_{i1} = t_{\text{cable}_i} - t_{\text{cable}_1}$, then the general expression of the TDOA can be written as

$$t_{i0} - t_{10} = t_i - t_1 - K_{i1} \quad (i = 2,3,\ldots,M), \tag{25}$$

where M denotes the number of used antennas. Moreover, throughout this experimental part, Antenna 1 (receiving) is considered the reference antenna.

Once the delays are estimated, we use an appropriate algorithm to estimate the coordinates of the mobile transmitter. The method described in [4], among other methods, can be used to perform the estimation. We are only interested in the step involving the estimation of TOA, and we compare the performance of the proposed approach to those proposed in the literature. We estimate the TDOA and the location along the trajectory containing 26 positions; 10 measurements of the received signal are made at each position, which allows having 30 TDOA values per position. The trajectory and the positions of the antennas are shown in Fig. 9.

A. LOS Channel Case

Now, we are interested in estimating the position of the mobile transmitter. The same estimation framework is kept for all algorithms except when estimating the TDOA values. We assess the performance of the HOTEST algorithm by comparing it to the performance of the CA-CFAR-based algorithm.

Figure 10 depicts the RMSE variation versus the SNR using

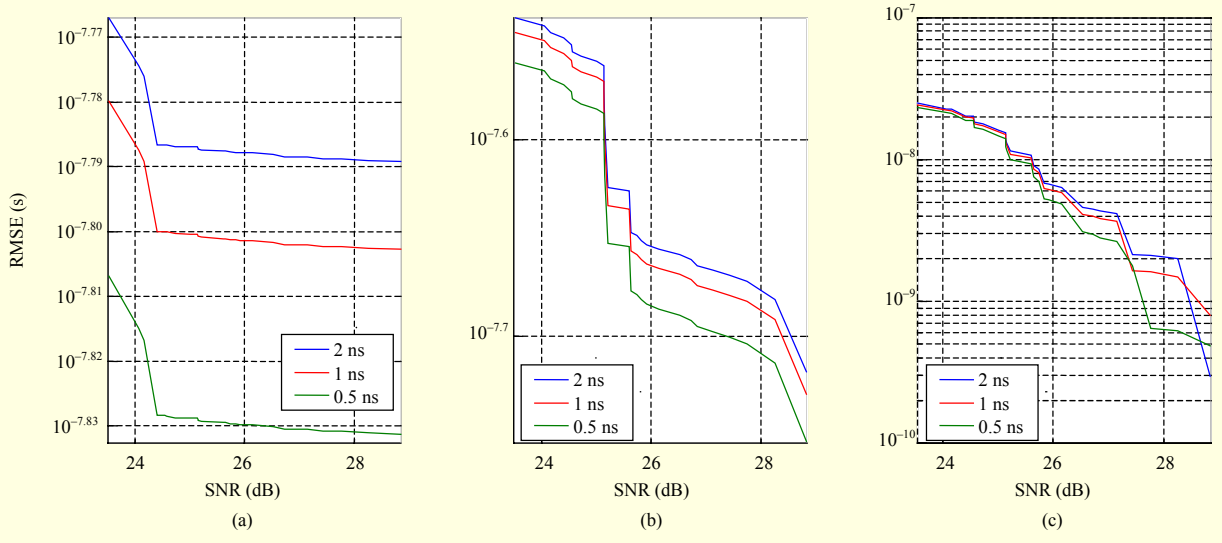

Fig. 10. T_b influence on TOA estimation: (a) t_1, (b) t_2, and (c) t_3.

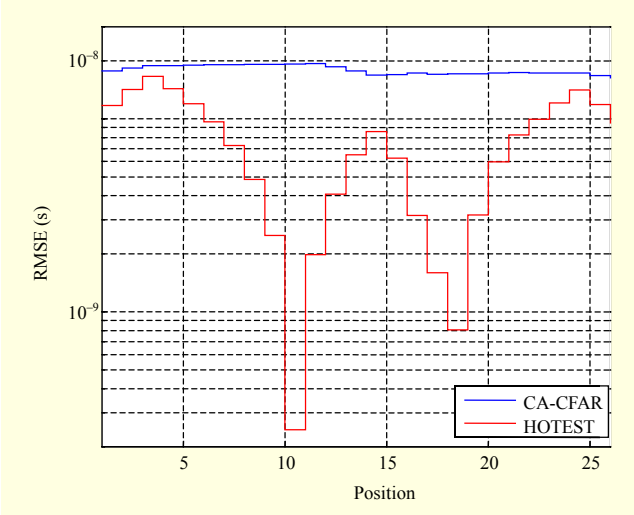

Fig. 11. Performance comparison of HOTEST vs. CA-CFAR-based algorithm for $T_b = 1$ ns and $N_b = 50$.

HOTEST algorithm for the set of parameters ($N = 20$ samples; N_b=50 for the first two values of T_b and N_b=17 for the last one). The abrupt changes observed in the estimation of t_2 are mainly due to the large variation in distance between the mobile transmitter and Antenna 2 (a jump of 5 m to 8 m). Figure 11 depicts the comparison of the algorithms and highlights the superiority of the proposed technique for providing a precise position of the mobile transmitter. This is due mainly to the easy detection of the abrupt changes in the statistical test.

B. NLOS Channel Case

Now, we consider the case of the absence of a direct LOS between the antennas. A metallic barrier is placed between the transmitter and Antenna 2. This obstacle does not allow signals to pass, except those diffracted by or reflected from the floor.

We compute the average SNR for each position of the mobile transmitter. Figure 12 shows that the presence of obstructions between Antenna 2 and the mobile transmitter results in the SNR decreasing by about 10 dB.

We repeat the same simulation framework for the NLOS case as in the LOS case. Figure 13 shows a comparison of HOTEST and the CA-CFAR-based estimation. The performance of the proposed approach is shown to be superior.

The superiority of HOTEST is mainly due to the fact that the decision is made based on distance $\hat{D}$ as a test statistic rather than directly on the values of the samples or their energies. In fact, detection based on the abrupt change of the distance measure is less sensitive to an increase in the noise power.

Observing the expressions of the distribution of the statistical test under H_1 (signal-plus-noise frame) in (17), the distance is of a factor of $\sqrt{N}$, and, under H_0 (noise-only frame) in (18),

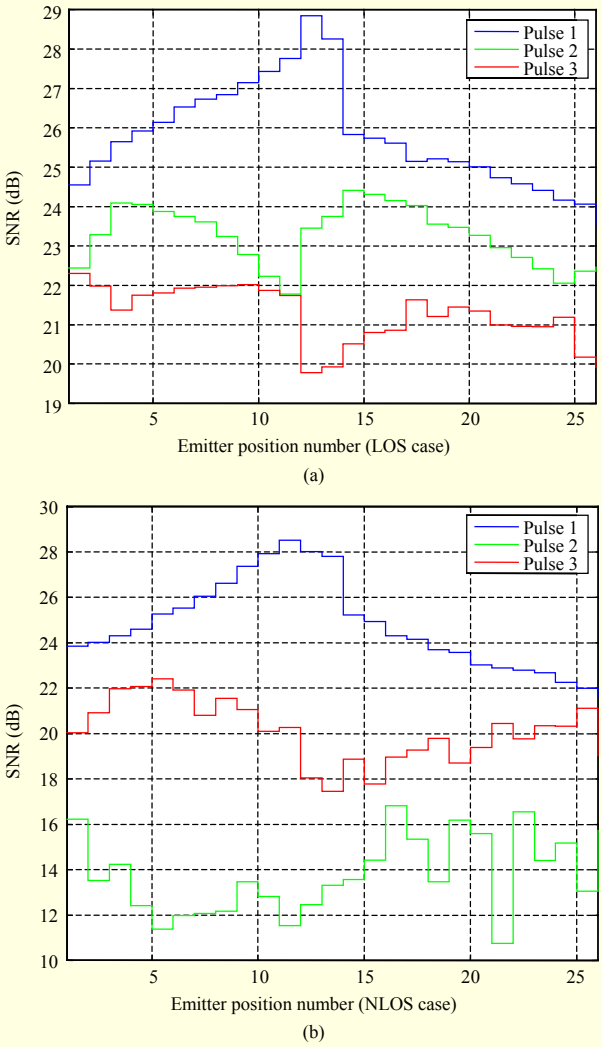

Fig. 12. SNR estimation for (a) LOS and (b) NLOS case.

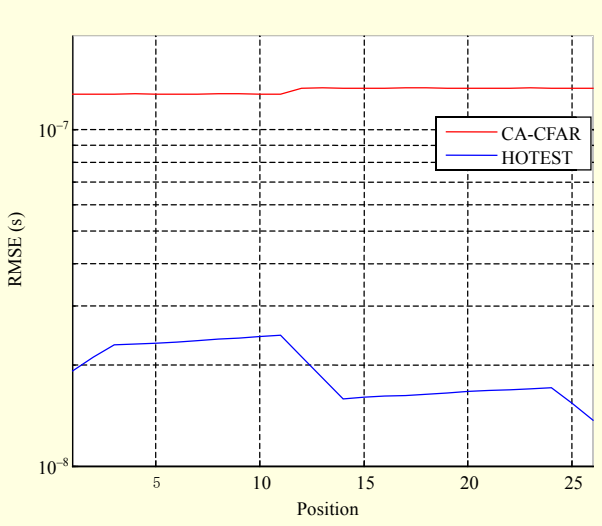

Fig. 13. HOTEST vs. CA-CFAR performance comparison.

the distance is of a factor of N. Hence, the transition from one model to another involves the detection of an abrupt change of $\sqrt{N}$. Also, by expressing the probability of detection in (20) (see [14] for more details of the derivation), we obtain

$$P_{\mathrm{d}} = Q(-N^{\frac{1}{2}}\frac{\hat{D}}{v^{1/2}} + \frac{2S_{\alpha}}{N^{1/2}v^{1/2}}), \tag{26}$$

where $Q(x) = \frac{1}{\sqrt{2\pi}}\int_{x}^{+\infty} e^{-\frac{t^2}{2}}dt$ and v is the variance of the normal distribution. The probability of detection reaches unity at a ratio of $N^{1/2}$.

3. Complexity Issue

The computation load of the HOTEST algorithm mainly corresponds to the AR coefficients derivation and the variance computation. It is around $(2p_x^3 - 4p_x^2 + 2p_x)/3$ multiplications for the Levinson-Durbin algorithm and the power spectral density computation for the frame under consideration. Generally, a value of p_x = 2 or 3 is enough to obtain a suitable performance.

A fair comparison between the proposed algorithm and the methods proposed in the literature is difficult to conduct because the frameworks and key parameters are different. In the MESSB algorithm, the first operation consists of an average computation of the received samples. Then, energy blocks are computed at the output of the ED receiver. The TOA is estimated after a search back and comparison against a threshold.

For the CA-CFAR-based technique, the main computation load is related to the computation of the variance of the noise on both sides of the block under test (BUT). Two frames are taken in both sides of the BUT, and an interval guard is kept between the frames and the BUT. The variance computation consumes (2N+2) multiplications, where N is the number of samples contained in the frame. CA-CFAR and MESSB involve the use of an empirical scale factor and an empirical threshold, respectively, which is not the case for HOTEST, wherein the threshold is obtained via a lookup table.

V. Conclusion

In this paper, a new method of estimating TOA in IR-UWB systems was proposed. The new method is based upon the homogeneity measure between two AR processes and has the advantage of presenting a threshold that is fixed analytically. The performance studies conducted through simulations and real-data experiments showed that the approach provides more accurate results than the TC, MESSB, and CA-CFAR algorithms, which were proposed in the literature. Additionally, the operations performed during TOA estimation are highly recommended for implementation in DSP or FPGA support, as the involved operations can be parallelized or pipelined.

Acknowledgment

The authors are very grateful to the reviewers and wish to express their gratitude for the constructive comments they provided to improve the quality and the readability of the paper.

References

[1] S. Gezici et al., "Localization via Ultra-wideband Radios: A Look at Positioning Aspects for Future Sensor Networks," *IEEE Signal Process. Mag.*, vol. 22, no. 4, 2005, pp. 70-84.

[2] J. Ni et al., "Ultra-wideband Time-Difference-of-Arrival High Resolution 3D Proximity Tracking System," *IEEE/ION Position, Location, Nav. Symp. (PLANS)*, 2010, pp. 37-43.

[3] L. Zheng, Z. Liu, and M. Wang, "Synchronization for IR-UWB System Using a Switching Phase Detector-Based Impulse Phase-Locked Loop," *ETRI J.*, vol. 34, no. 2, Apr. 2012, pp. 175-183.

[4] J. Ni and R. Barton, "Design and Performance Analysis of a UWB Tracking System for Space Applications," *IEEE/ACES Int. Conf. Wireless Commun. Appl. Comput. Electromagn.*, 2005, pp. 31-34.

[5] I. Guvenc and Z. Sahinoglu, "Threshold-Based TOA Estimation for Impulse Radio UWB Systems," *IEEE Int. Conf. Ultra-Wideband*, 2005, pp. 420-425.

[6] T.C. Liu, D.I. Kim, and R.G. Vaughan, "A High-Resolution, Multi-Template Deconvolution Algorithm for Time-Domain UWB Channel Characterization," *Canadian J. Electric. Comput. Eng.*, vol. 32, no. 4, 2007, pp. 207-213.

[7] J.Y. Lee and R.A. Scholtz, "Ranging in a Dense Multipath Environment Using an UWB Radio Link," *IEEE J. Sel. Areas Commun.*, vol. 20, no. 9, 2002, pp. 1677-1683.

[8] R. Badorrey et al., "Evaluation of TOA Estimation Algorithms in UWB Receivers," *14th European Wireless Conf.*, 2008, pp. 1-6.

[9] A. Maali et al., "Adaptive CA-CFAR Threshold for Non-Coherent IR-UWB Energy Detector Receivers," *IEEE Commun. Lett.*, vol. 13, no. 12, 2009, pp. 959-961.

[10] B. Shen et al., "Rayleigh-Quotient and Iterative-Threshold-Test-Based Blind TOA Estimation for IR-UWB Systems," *ETRI J.*, vol. 32, no. 2, Apr. 2010, pp. 333-345.

[11] N. Levinson, "The Wiener RMS (Root-Means-Square) Error Criterion in Filter Design and Prediction," *J Math. Phys.*, vol. 25, 1947, pp. 261-278.

[12] J. Durbin, "The Fitting of Time-Series Models," *Rev. Int. Statist. Instit.*, vol. 28, no. 3, 1960, pp. 233-244.

[13] H. Akaike, "A New Look at the Statistical Model Identification," *IEEE Trans. Autom. Contr.*, vol. 19, no. 6, 1974, pp. 716-723.
[14] K. Drouiche, "Testing Proportionality for Autoregressive Processes," *IEEE Trans. Inf. Theory*, vol. 49, no. 3, 2003, pp. 672-681.
[15] A. Maali et al., "UWB Localization System with TDOA Algorithm Using Experimental Measurements," *3rd Int. Conf. Adv. Satellite Space Commun.*, 2011, pp. 97-102.
[16] Time Domain Corporation, *PulsON 210™ Getting Started Guide*, 2005.
[17] Time Domain Corporation, *PulsON P210 Reference Design*, product brochure. Available: http://www.timedomain.com/products/P2101RD.pdf

Mustapha Djeddou received his MS in 1998 and his PhD with highest honor in electrical engineering in 2005, both from the National Polytechnic School, Algiers. Currently, he is the head of the Communication Systems Laboratory at the Military Polytechnic School, Algiers. His research interests include biometrics, statistical signal processing, applied signal processing for digital communication, and wireless communication.

Hichem Zeher received his MS in 2012 from the Military Polytechnic School, Algiers. Currently, he is with the Communication Systems Laboratory, Military Polytechnic School, Algiers. His research interests are signal processing, applied mathematics, and signal processing for digital communication.

Younes Nekachtali is with the Communication Systems Laboratory, Military Polytechnic School, Algiers. He received his MSc in 2012 from the Military Polytechnic School. Currently, he is working toward his PhD His research interests include signal estimation and detection and array signal processing.

Karim Drouiche obtained his engineering diploma in 1988 at USTA, Algiers, and his PhD in 1993 from École Nationale Supérieure des Télécommunications, Paris, France. Currently, he is a researcher at Cergy University, France. His main interests are signal processing and statistics.